Effect of Copper Doping on Physical Characteristic of Cobalt Oxide Nanostructured Thin Films Deposited for Gas Sensing

Fikrat Hikmat Jasim[1], Abeer Ghalib Hadi[2], Tahseen Hussain Mubarak[3], Muhaned Zaidi[4], Farah Abdulrazzaq Jasim[1] and Muhannad Jadan[5]
[1]*Department of Physics, College of Education, Mustansiriyah University, 10052 Baghdad, Iraq*
[2]*General Directorate of Education in Baghdad Governorate - Rusafa Second, Ministry of Education, 10001 Baghdad, Iraq*
[3]*Department of Physics, College of Science, University of Diyala, 32001 Diyala, Iraq*
[4]*Department of Medical Physics, College of Science, Al-Manara University, 62001 Amarah, Iraq*
[5]*Department of Applied Physics, Faculty of Science, Tafila Technical University, PO Box 179, 66110 Tafila, Jordan*
Farah.A.j@uomustansiriyah.edu.iq

Keywords: Co_3O_4, Cu, SPM, Structural Properties, Optical Band Gap, NO_2 Gas Sensing.

Abstract: (Co_3O_4: Cu) nanostructured films were deposited by the chemical spray pyrolysis (CSP) method. XRD analysis assure a polycrystalline cubic structure with peak at (220) plane. Improved crystalline quality was demonstrated by the crystallite size increasing from 16.96 nm for undoped films to 27.82 nm for 3% Cu-doped samples, and the dislocation density decreasing from 39.74×10^{12} to 30.41×10^{12} lines/m². Surface alteration was detected by AFM, and the average particle size decreased from 68.6 nm to 32.6 nm after dopingAs Cu content rose, optical transmittance in the visible range dropped from 85.5% to 80.6%, whereas absorbance steadily increased. Due to defect-state formation within the band structure, the direct optical bandgap decreased from 2.50 eV to 2.40 eV. Strong light absorption was confirmed by the absorption coefficient exceeding 10^cm⁻¹. Because of structural alterations, the refractive index dropped as the Cu content increased. Copper doping greatly affected sensor response, as seen by gas-sensing experiments for NO_2 at 80°C. Sensitivity dropped from 53.62% for undoped Co_3O_4 to 29.43% for 3% Cu-doped films at 220 ppm, demonstrating decreased sensitivity at higher doping levels.

1 INTRODUCTION

Co_3O_4 thin films have garnered a lot of attention from researchers because of their potential uses in a variety of technical fields, such as use as negative electrode materials in lithium-ion batteries [1], [2], as anodic electrochromic layers for smart windows [3], [4], and as high-temperature solar selective absorbers [5], [6]. Co_3O_4 exhibits a spinel crystal structure characterized by intrinsic cation vacancies that enhance its chemical stability. This unique structural feature endows Co_3O_4 with exceptional properties that render it highly suitable for various electrochemical applications [8]-[10]. Several deposition techniques were used to create Co_3O_4, like RF magnetron sputtering [11], ALD [12], CBD [13], sol-gel processing [14], co-precipitation [15], PLD [16], CBD [17], and SPM [18]. Due to its potential for user-friendliness, low initial cost, and the capacity to deposit uniform thin films across a large surface with strict control over composition and thickness, SPM has garnered a lot of attention [19]-[24]. The sensing applications of Undoped Co_3O_4 thin films are impacted by their modest sensitivity and weak electrical conductivity [25]-[27]. Copper incorporation in Co_3O_4 thin films drastically alters the structural, optical, and sensing properties [28]. In this work, Cu-doped Co_3O_4 nanostructured thin films were developed via CSP, and the effect of copper doping on their structural, optical, and sensing properties was studied.

2 EXPERIMENTAL

Co_3O_4 film: Co_3O_4 was synthesized through the CSP method. The membranes were created by decomposing a 0.1 M solution of ($CoCl_2.6H_2O$) in 100 ml of redistilled water. The volume fractions used for copper chloride were 1% and 3%. The optimization parameters established in this study indicated that the substrate should be maintained at 450 °C. The solution prepared was sprayed onto glass bases. The spray rate was set at 0.2 ml per spray, with a sprayer nozzle height of 28 cm. Each spray lasted 8 seconds, and the interval between consecutive sprays was 2 minutes, while the nitrogen carrier gas was maintained at 105 Pa. The target thickness was 340 ± 25 nm. The structural properties of the deposited films were examined using XRD. Surface topography was investigated with an AFM. A dual-beam spectrophotometer from Shimadzu, Japan, was used to measure transmittance over the wavelength range of 380-900 nm. Studies of gas sensitivity were usually carried out in a cylinder laboratory chamber that sized 16 cm in height and 8 cm in radius.

3 RESULTS AND DISCUSSION

XRD patterns of the Co_3O_4 thin films are presented in Figure 1. According to the ICDD database (Card No. 42-146), the diffraction peaks noticed at 2θ values of 31.38°, 37.52°, 54.62°, and 65.57° linked to (220), (311), (422), and (440) crystallographic planes, respectively. These results indicate that the films display a predominantly hexagonal structure, with the (220) plane representing the preferred orientation.

Average crystallite size (D) was calculated from the diffraction peak's full width at half maximum (β), the X-ray wavelength (λ), and the Bragg angle (θ) using the Scherrer equation [29], [30].
D ranged from 16.96 to 27.82 nm, demonstrating a significant improvement in crystallinity; this could be linked to the effect of copper doping [14].

Dislocation density (δ), which is inversely proportional to the square of the crystallite size, was determined following [31].

δ of Co_3O_4 films decreases from 39.74 × 10^{14} lines/m² in the undoped sample to 30.42 × 10^{14} lines/m² in the film doped with 3% Cu. This drop implies fewer lattice defects, indicating that Cu incorporation improves crystalline quality and enhances the material's structural stability, which in turn can influence its electronic and optical properties [32].

The strain (ε), which quantifies lattice distortions within the crystallites, was estimated from the crystallite size and diffraction peak broadening [33].
ε decreases from 26.43 × 10^{-4} for undoped samples to 17.72 × 10^{-4} for films doped with 3% Cu, as shown in Table 1. This reduction in strain suggests that Cu incorporation alleviates lattice distortions, thereby improving crystallinity [34]. The structural parameters (S_{par}) comprising D, δ, and ε are listed in Table 1. Figure 2 depicts the variability of FWHM, D, δ, and ε versus Cu doping.

AFM was used to analyze surface topography of Co_3O_4 and Co_3O_4 films doped with 1% Cu. The images shown in Figure 3 disclose granular structures with surface scattering. Surface morphology roughness (Ra) and root mean square roughness (RMS) were investigated. As illustrated in Figure 3, Cu doping significantly influenced surface characteristics, resulting a changes in average particle size Pav, Ra, and RMS values, which were measured as (68.6, 61.8, 32.6) nm, (8.35, 6.52, 4.61) nm, and (7.65, 4.63, 3.27) nm, respectively [34]. Table 2 verifies that Cu incorporation reduces RMS, Ra and Pav of the films. These findings imply that Cu dopants promote particle growth and alter surface texture.

Figure 4 shows transmittance (T) spectra of Co_3O_4 films. In the Vis area, T ranges from 85.5% to 80.6%. A higher T is noted at longer wavelengths, showing a decrease in light absorption in NIR area, suggesting that films permit more efficient transmission [35].

Table 1: Structural parameters and optical band gap of undoped and Cu-doped Co_3O_4 thin films.

Sample	(hkl) Plane	2 θ (°)	FWHM (°)	E_g (eV)	*D* (nm)	δ × 10^{14} (lines/m²)	ε × 10^{-4}
Undoped Co_3O_4	220	31.38	0.74	2.50	16.96	39.74	26.43
Co_3O_4 :1% Cu	220	31.34	0.70	2.45	22.34	38.25	20.69
Co_3O_4 :3% Cu	220	31.31	0.66	2.40	27.82	30.41	17.72

Table 2: AFM surface parameters of undoped and Cu-doped Co_3O_4 thin films.

Sample	P_{av} nm	Ra (nm)	RMS (nm)
$Co_3O4_{Undoped}$	68.6	8.35	7.65
Co_3O_4 :1% Cu	61.6	6.52	4.63
Co_3O_4 :3% Cu	32.6	4.61	3.27

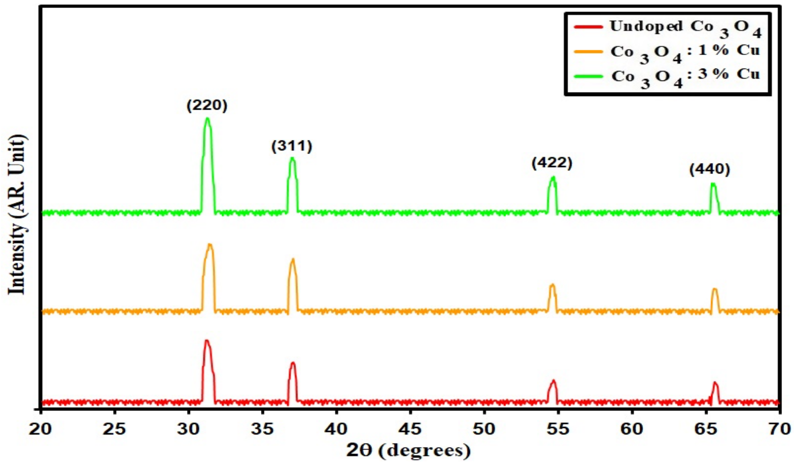

Figure 1: XRD patterns of undoped and Cu-doped Co_3O_4 thin films.

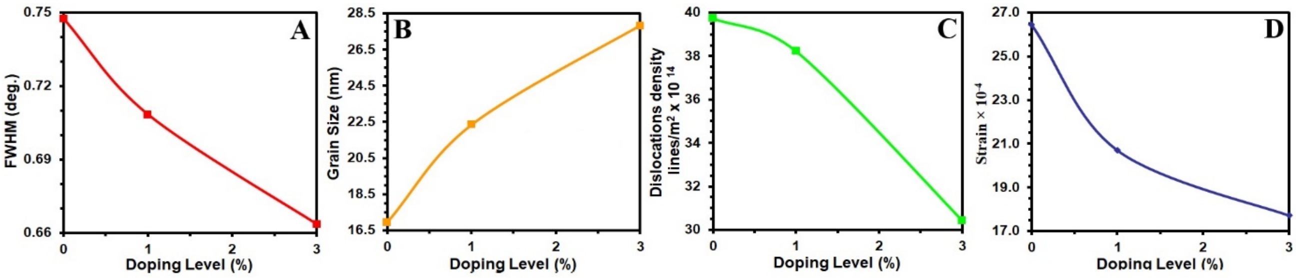

Figure 2: Variation of structural parameters (FWHM, crystallite size, dislocation density, and lattice strain) with Cu doping concentration.

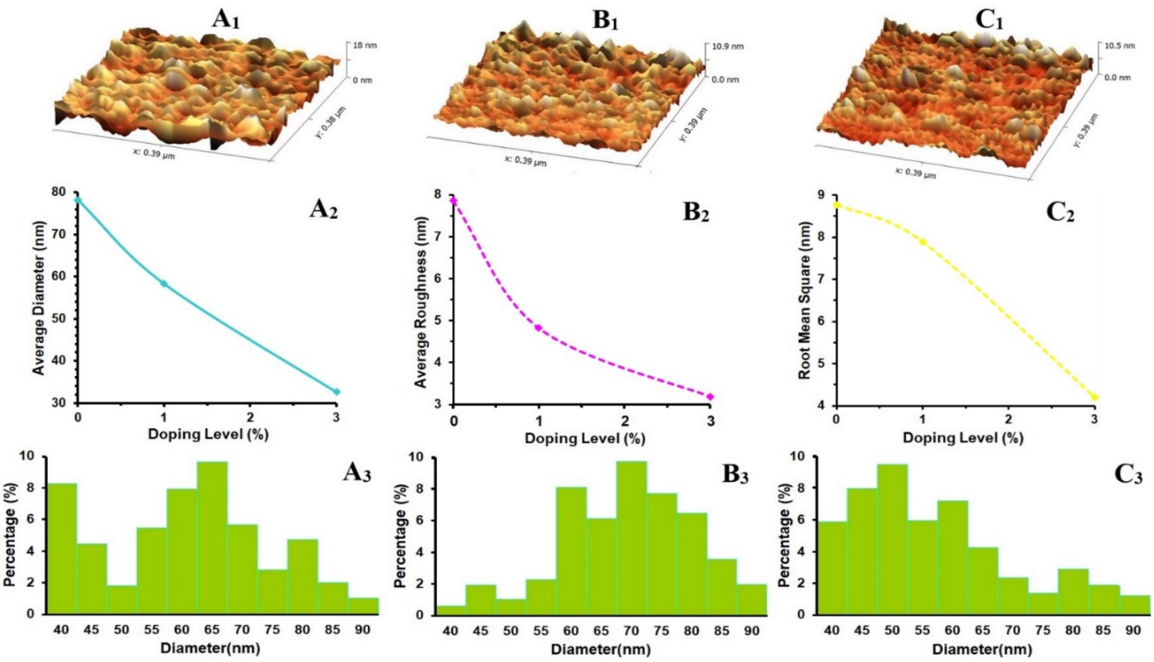

Figure 3: AFM surface morphology of undoped and Cu-doped Co_3O_4 thin films.

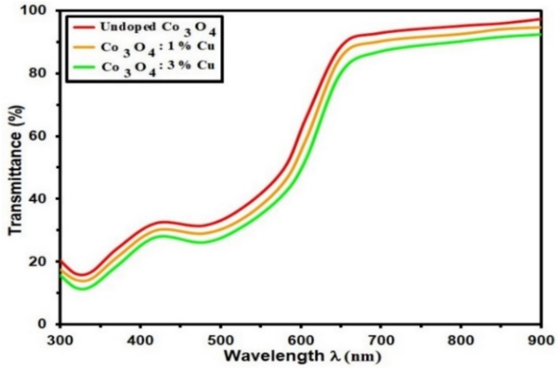

Figure 4: Optical transmittance spectra of undoped and Cu-doped Co_3O_4 thin films.

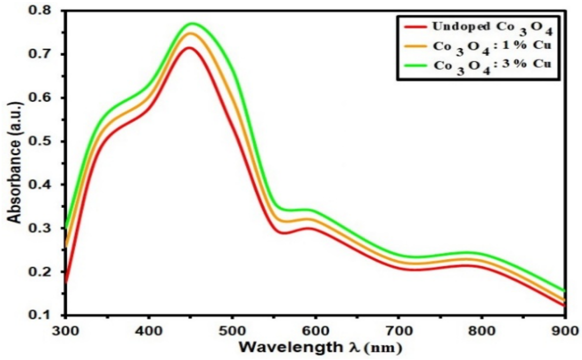

Figure 5: Optical absorbance spectra of undoped and Cu-doped Co_3O_4 thin films.

Absorbance (A) was evaluated from the transmittance (T), based on the intensity of transmitted light (I) and incident light (I_0) [36].

A is presented in Figure 5. The Co_3O_4 film shows the lowest A, while films doped with 1% and 3% Cu exhibit higher A. The increase in A is mostly ascribed to the incorporation of Cu ions, which introduce additional electronic states within the Co_3O_4 lattice [37].

The absorption coefficient (α) was obtained from the absorbance and film thickness (t) [38], [39].

Figure 6 shows that α initially rises sharply and then gradually decreases at higher energies. The high values of α (≥ 10^{-4} cm^{-1}) indicate strong light absorption and efficient direct electronic transitions within Co_3O_4 films. The observed enhancement of α with Cu inclusion suggests improved photon absorption efficiency, which can be ascribed to the formation of new defect states [40], [41].

The direct bandgap (Eg) was determined from the Tauc relation between the absorption coefficient and photon energy, taking n = 1/2 for a direct allowed transition [42].

Figure 7 illustrates that Eg of Co_3O_4 films decreased with increasing Cu content. This reduction is ascribed to Cu-induced defect states, which introduce additional energy levels within Eg. Consequently, Eg of Co_3O_4 declined from 2.50 eV to 2.40 eV at the highest Cu doping level. The observed narrowing of Eg can be explained by the increased structural disorder and higher defect density induced by Cu incorporation, which alter the electronic structure and facilitate easier electronic transitions [43], [44].

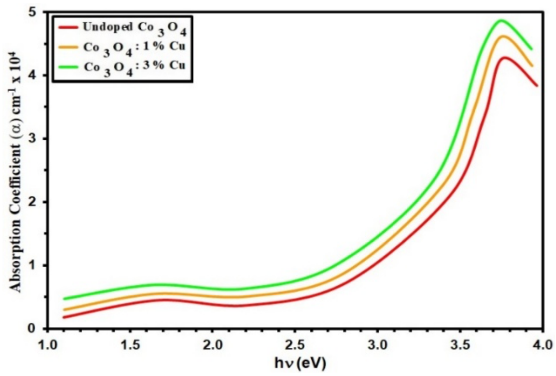

Figure 6: Absorption coefficient (α) as a function of photon energy (hν) for undoped and Cu-doped Co_3O_4 thin films.

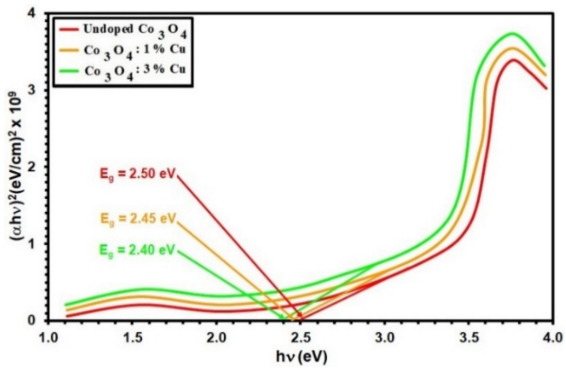

Figure7: Tauc plots ($(\alpha h\nu)^2$ versus hν) of undoped and Cu-doped Co_3O_4 thin films.

The extinction coefficient (k) was calculated from the absorption coefficient (α) and wavelength (λ) [45].

As shown in Fig. 8, k tends to rise rapidly in the ultraviolet (UV) region before declining, even at photon energies (hν) below the fundamental absorption edge, which suggests that impurities or defect states in the film cause some absorption [46].

The refractive index (n) was computed from the reflectance (R) and extinction coefficient (k) [47].

Figure 9 displays n of Undoped Co3O4 films as a function of wavelength. All Co3O4:Cu films have a refractive index that is directly correlated with wavelength. Additionally, as copper content increases, the refractive index decreases. This drop in (n) at higher doping concentrations can be accounted for by changes in electrical polarizability and structural alterations induced by copper incorporation, which affect the material's capacity to transmit light [48], [49].

At 80°C, the gas sensing properties were evaluated. The resistance (R) change when exposed to (NO_2) gas at a 200-ppm concentration is shown in Figure 10. Undoped Co_3O_4 films were found to have the lowest R, suggesting better adsorption of NO_2 molecules [50]. On the other hand, the Undoped Co_3O_4 films doped with 3% copper exhibited the highest R. This implies that copper doping increases R) and alters the gas-sensing properties of Undoped Co_3O_4 films [51]-[53]. Sensitivity was then determined from the relative change in resistance between air and gas exposure [54], [55].

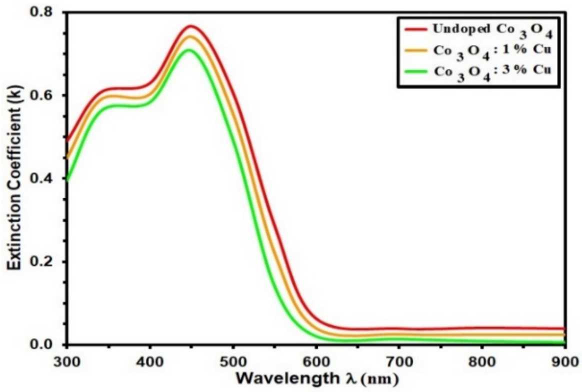

Figure 8: Extinction coefficient spectra of undoped and Cu-doped Co_3O_4 thin films.

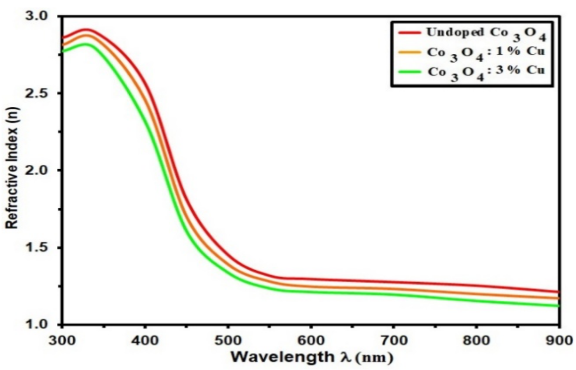

Figure 9: Refractive index spectra of undoped and Cu-doped Co_3O_4 thin films.

Ra represents the resistance in air and Rg represents the film sensor's resistance in the presence of gas. The sensitivity curves showing the effects of undoped Co3O4, Co3O4: 1% Cu, and Co3O4: 3% Cu upon exposure to NO2 gas are shown in Figure 11. The sensitivity is affected by charge carrier recombination between electrons and holes, which decreases with increasing copper doping concentration. In particular, the sensitivity decreases from 49.21% to 26.43% at 120 ppm, from 51.54% to 27.89% at 170 ppm, and from 53.62% to 29.43% at 220 ppm for undoped Co3O4, Co3O4: 1% Cu, and Co3O4: 3% Cu. This drop in sensitivity indicates that higher copper concentrations make the sensor less sensitive to NO2 [56], [57]. This effect is explained by structural changes, which affect the sensor's performance [58]-[60].

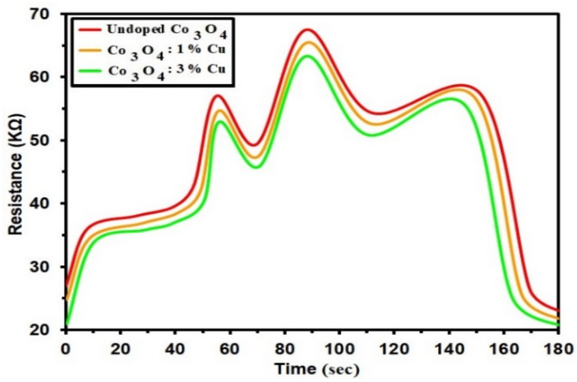

Figure 10: Resistance response of undoped and Cu-doped Co_3O_4 thin films under NO_2 gas exposure.

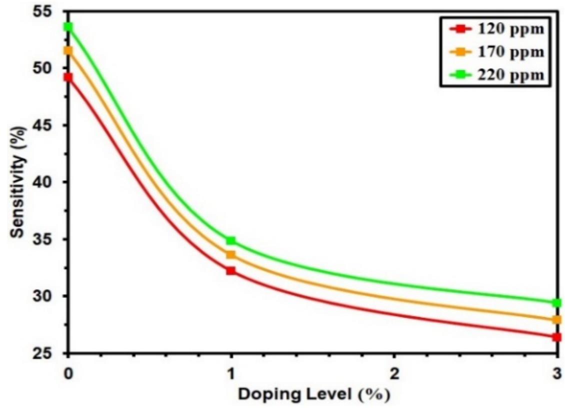

Figure 11: NO_2 gas sensitivity of undoped and Cu-doped Co_3O_4 thin films.

4 CONCLUSIONS

In this study, undoped and Cu-doped Co_3O_4 nanostructured thin films were successfully synthesized via SPM at 450°C. XRD analysis confirmed that all films are polycrystalline with a cubic structure and exhibit a strong peak along the (220) plane. *D* increased from 16.96 nm to 27.82 nm while reducing dislocation density and microstrain. AFM findings proved that average particle size and surface roughness were reduced. The transmittance decreased with increasing Cu concentration, while absorbance. The optical bandgap narrowed from 2.50 eV for Co_3O_4 to 2.40 eV for 3% Cu-doped films. Additionally, n decreased with higher Cu content. Gas-sensing tests for NO_2 at 80°C proved that sensitivity decreased from 53.62% to 29.43% at 220 ppm with increasing Cu doping.

ACKNOWLEDGMENTS

The authors gratefully acknowledge the financial and institutional support provided by Mustansiriyah University (www.uomustansiriyah.edu.iq) for this research.

REFERENCES

[1] W. Shen, P. Liu, L. Wang, H. Yang, J. Chen, F. Chen, et al., and X. Xia, "Research Progress on Halide Solid-State Electrolytes: Synthesis, Mechanism, and Modification," Carbon Energy, e70170, 2026.

[2] R. Dhahiya, Dinesh, M. Gupta, P. Rajput, P. Sharma, and A. Kumar, "Electrochemical Supercapacitors Based on Pseudocapacitance," in Handbook of Energy Materials in Supercapacitors and Storage Devices, pp. 35-64, 2026.

[3] N. A. H. Hashim and T. A. Al-Mashhadani, "Optoelectronic Characteristics of Co3O4 NPs/PSi/Si Photodetector," Iraqi Journal of Applied Physics Letters, vol. 9, no. 1, pp. 34-37, 2026.

[4] P. Jebin, M. R. Khan, S. S. Shah, N. Debnath, M. A. Aziz, B. J. Kim, and A. S. Ahammad, "Synergistic Integration of Quantum Materials with Smart Electrolytes for Next-Generation Multifunctional Supercapacitors: Advances, Challenges, and Future Prospects," Small, vol. 22, no. 8, e08559, 2026.

[5] F. Xu, L. Zheng, J. Zhang, Y. He, H. Cao, X. Zheng, et al., and J. Yu, "Co3O4 as Full-Solar-Spectrum Photocatalyst for Selective Methane Conversion Through Reactive Oxygen Species Control," Nature Catalysis, pp. 1-14, 2026.

[6] H. Duaa Jabbar, "Preparation of Nano-Oxides for Photovoltaic Applications by Drop-Casting," Preparation of Nano-Oxides for Photovoltaic Applications by Drop-Casting, vol. 4, no. 3, pp. 22-29, 2026.

[7] D. M. Stansel, N. M. Laurendeau, and D. W. Senser, "CO and NOx Emissions from a Controlled-Air Burner: Experimental Measurements and Exhaust Correlations," Combustion Science and Technology, vol. 104, no. 4-6, pp. 207-234, 1995.

[8] N. Bhuvanendran, M. G. Choi, D. Kim, and S. Y. Lee, "Improved Trifunctional Electrocatalytic Performance of Integrated Co3O4 Spinel Oxide Morphologies with Abundant Oxygen Vacancies for Oxygen Reduction and Water-Splitting Reactions," Journal of Alloys and Compounds, vol. 935, 168079, 2023.

[9] G. El Haber, F. Goutaland, D. Luneau, D. Jamon, J. P. Chatelon, J. Y. Michalon, et al., and F. Royer, "Magneto-Optical Properties of Cobalt and Co3O4 Thin Films: Influence of Microstructural Properties," Journal of Applied Physics, vol. 137, no. 12, 2025.

[10] Y. Su, H. Liu, C. Li, J. Liu, Y. Song, and F. Wang, "Hydrothermal-Assisted Defect Engineering in Spinel Co3O4 Nanostructures as Bifunctional Catalysts for Oxygen Electrode," Journal of Alloys and Compounds, vol. 799, pp. 160-168, 2019.

[11] H. Ot, B. Akaoglu, and A. B. D. U. L. L. A. H. Yildiz, "Tuning Carrier Transport and Optical Properties of Co3O4 Thin Films via Sputtering Power," Journal of Alloys and Compounds, 186312, 2026.

[12] V. Prathipa, A. U. Devi, M. A. Wadaan, T. Kamatchi, and A. Roniboss, "A Volatile Cobalt (II) Complex as a Precursor for Nanostructured Co3O4 Thin Films via PA-MOCVD: Synthesis, Vapor Pressure Study, and Structural Analysis," Journal of Materials Science: Materials in Electronics, vol. 36, no. 18, p. 1079, 2025.

[13] S. L. Bee, C. W. Ooi, S. Y. Pung, S. L. Chiam, C. P. Leo, and W. K. Tan, "In Situ Synthesis and Immobilization of Co3O4 Nanowalls on Kanthal Substrate Using a Rapid Direct Heating Approach," Materialia, vol. 42, 102457, 2025.

[14] Himanshu and R. Kumar, "Review of Cobalt Oxide (CoO) Thin Films Prepared by Various Techniques," in Journal of Physics: Conference Series, vol. 2267, no. 1, p. 012002, IOP Publishing, 2022.

[15] A. M. Abdulwahab, T. S. Aldeen, S. N. Aziz, and A. A. Ahmed, "Design and Photocatalytic Evaluation of CdO-ZnO-Co3O4 Ternary Nanocomposite Synthesized by Co-Precipitation Method," Thamar University Journal of Natural & Applied Sciences, vol. 10, no. 1, pp. 16-24, 2025.

[16] M. S. Mahmood, N. K. Hassan, and W. M. Mohammed, "Photodetection Performance Enhancement of Crystal-Like Co3O4 Nanostructure Synthesized via Pulsed Laser Deposition," International Journal of Nanoelectronics and Materials (IJNeaM), vol. 18, pp. 119-124, 2025.

[17] G. W. Kumarage, S. Jayawardena, D. Zappa, M. Shimomura, and E. Comini, "Unlocking Superior Acetone Sensitivity with Co3O4/ZnO Nanowire Innovations," Sensors and Actuators B: Chemical, vol. 431, 137450, 2025.

[18] H. Ghannam, I. Oumouna, and A. Chahboun, "Influence of Deposition Time on the Structural, Optical, and Electrochemical Properties of Sprayed Co3O4 Thin Films," Next Materials, vol. 10, 101364, 2026.

[19] N. Vervoort, K. Goossens, M. Baeten, and Q. Chen, "Recent Advances in Analytical Techniques for High Throughput Experimentation," Analytical Science Advances, vol. 2, no. 3-4, pp. 109-127, 2021.

[20] B. Ramasubramanian, S. Sundarrajan, R. P. Rao, M. V. Reddy, V. Chellappan, and S. Ramakrishna, "Novel Low-Carbon Energy Solutions for Powering Emerging Wearables, Smart Textiles, and Medical Devices," Energy & Environmental Science, vol. 15, no. 12, pp. 4928-4981, 2022.

[21] T. Zhou, Z. Qiu, Y. Li, Y. Ma, W. Tao, B. Dong, et al., and H. Li, "Wire Arc Additive Manufacturing of Nickel-Based Superalloy and Stainless Steel Dissimilar Material Component," in Materials for Land, Air, and Space Transportation, CRC Press, pp. 334-386, 2024.

[22] X. C. Huang, J. Y. Zhang, M. Wu, S. Zhang, H. Y. Xiao, W. Q. Han, et al., and K. H. L. Zhang, "Electronic Structure and p-Type Conduction Mechanism of Spinel Cobaltite Oxide Thin Films," Physical Review B, vol. 100, no. 11, 115301, 2019.

[23] H. Zhang, S. Pokhrel, Z. Ji, H. Meng, X. Wang, S. Lin, et al., and A. E. Nel, "PdO Doping Tunes Band-Gap Energy Levels as Well as Oxidative Stress Responses to a Co3O4 p-Type Semiconductor in Cells and the Lung," Journal of the American Chemical Society, vol. 136, no. 17, pp. 6406-6420, 2014.

[24] A. Miquelot, M. Despotopoulou, C. Vahlas, C. Villeneuve, N. Dragoe, N. Prud'Homme, and O. Debieu, "Morphological, Structural, Optical, and Electrical Study of Nanostructured Thin Films: Charge Transport Mechanism of p-Type Co3O4," Materials Chemistry and Physics, vol. 240, 122059, 2020.

[25] V. V. Petrov, V. V. Sysoev, I. O. Ignatieva, I. A. Gulyaeva, M. G. Volkova, A. P. Ivanishcheva, et al., and E. M. Bayan, "Nanocomposite Co3O4-ZnO Thin Films for Photoconductivity Sensors," Sensors, vol. 23, no. 12, p. 5617, 2023.

[26] P. Singh, R. Kumar, and R. K. Singh, "Progress on Transition Metal-Doped ZnO Nanoparticles and Its Application," Industrial & Engineering Chemistry Research, vol. 58, no. 37, pp. 17130-17163, 2019.

[27] T. Baran, A. Visibile, M. Busch, X. He, S. Wojtyla, S. Rondinini, et al., and A. Vertova, "Copper Oxide-Based Photocatalysts and Photocathodes: Fundamentals and Recent Advances," Molecules, vol. 26, no. 23, p. 7271, 2021.

[28] M. Zahan and J. Podder, "Synthesis and Characterizations of Cu-Doped Co3O4 Nanostructured Thin Films Using Spray Pyrolysis for Glucose Sensor Applications," Biointerface Research in Applied Chemistry, vol. 12, no. 5, pp. 6321-6335, 2022.

[29] M. Issa and K. A. Aadim, "Influence of Gas Flow Rate on the Plasma Temperature and Electron Density of an Atmospheric Argon Plasma Jet," Jordan Journal of Physics, vol. 18, no. 4, pp. 435-442, 2025.

[30] N. Y. Ahmed, B. A. Bader, M. Y. Slewa, N. F. Habubi, and S. S. Chiad, "Effect of Boron on Structural, Optical Characterization of Nanostructured Fe2O3 Thin Films," NeuroQuantology, vol. 18, no. 6, pp. 55-60, 2020.

[31] F. Tariq, M. M. Baig, S. T. Almutairi, S. G. Lee, I. Shakir, and M. F. Warsi, "Carbon Nanotubes Supported Bimetallic Doped Co3O4 Composite: A New Electrode Material for Evaluation of Electrochemical Energy Storage Properties," Journal of Alloys and Compounds, 183169, 2025.

[32] D. M. Mamand, D. S. Muhammad, S. B. Aziz, P. O. Hama, B. A. Al-Asbahi, A. A. Ahmed, and J. Hassan, "Enhanced Optical Properties of Chitosan Polymer Doped with Orange Peel Dye Investigated via UV-Vis and FTIR Analysis," Scientific Reports, vol. 15, no. 1, p. 3232, 2025.

[33] R. S. Ali, M. K. Mohammed, A. A. Khadayeir, Z. M. Abood, N. F. Habubi, and S. S. Chiad, "Structural and Optical Characterization of Sprayed Nanostructured Indium Doped Fe2O3 Thin Films," Journal of Physics: Conference Series, vol. 1664, no. 1, 012016, 2016.

[34] M. A. Issa and K. A. Aadim, "Optical and Structural Characterization of ZnO:NiO Nano Composite Prepared by Pulsed Laser Deposition Method," J Opt, vol. 54, pp. 2357-2362, 2025.

[35] D. Mahana, A. K. Mauraya, P. Singh, and S. K. Muthusamy, "Evolution of CuO Thin Films Through Thermal Oxidation of Cu Films Prepared by Physical Vapour Deposition Techniques," Solid State Communications, vol. 366, 115152, 2023.

[36] Z. Yuan, M. Zhang, X. Luo, and F. Meng, "In/Cu Co-Doped Porous Co3O4 Nanosheets for Enhanced Xylene Detection," IEEE Sensors Journal, vol. 25, no. 6, pp. 9323-9330, 2025.

[37] U. Chinnathambi, R. Chandrapal, A. R, B. Palanivel, and T. Kalaivani, "Copper-Enriched Co3O4/MoS2 Nanocomposites for Superior Photocatalytic Degradation of Methylene Blue Under Visible Light," Journal of Cluster Science, vol. 36, no. 2, p. 43, 2025.

[38] H. T. Salloom, E. H. Hadi, N. F. Habubi, S. S. Chiad, M. Jadan, and J. S. Addasi, "Characterization of Silver Content Upon Properties of Nanostructured Nickel Oxide Thin Films," Digest Journal of Nanomaterials and Biostructures, vol. 15, no. 4, pp. 1189-1195, 2020.

[39] A. Prakash, V. Mishra, and M. G. Mahesha, "Development of Enduring Interstitial Defects in Mg-Doped CuO Thin Films," RSC Advances, vol. 14, no. 14, pp. 10004-10016, 2024.

[40] M. Albarkani, I. H. Alsohaimi, M. S. Alhumaimess, M. Alzaid, Q. Chen, M. A. El-Hashemy, and H. M. Hassan, "Mitigating Electronic Limitations in Co3O4 via Rational Dopant Integration for Multifunctional Sustainable Energy Applications: Oxygen Evolution and Photoelectrochemical Water Reduction," Electrochimica Acta, 148085, 2025.

[41] D. Salmote, A. R. Pawar, K. R. Shaikh, and P. B. Undre, "Enhanced Photocatalytic Degradation of Crystal Violet with Hexagonal Nanosheets of Cu-Doped Co3O4 Under UV and Visible Irradiation," Journal of Materials Science: Materials in Electronics, vol. 36, no. 8, p. 473, 2025.

[42] M. A. Issa and K. A. Aadim, "Influence of Laser Energy on Structural and Optical Properties of ZnO(x):NiO(1−x) Films Prepared by Pulse Laser Deposition," J Opt, 2024.

[43] Y. X. Lin, D. S. Tsai, Z. Y. Chen, and C. P. Lee, "Enhanced Performance of Photocatalytic CO2 Reduction Using Cu@Graphene Nanoparticle-Decorated Co3O4 Nanoneedles," ChemElectroChem, vol. 12, no. 7, e202400689, 2025.

[44] S. Mahmood Hussein, Tahseen Hussain Mubarak, S. M. Ali Ridha, and J. Al-Zanganawee, "Synthesis and Characterizations of Nano Magnetic Particles (Co-Ni Fe2O4) Ferrite by Co-Precipitation and Biomedical Application," International Journal of Nanoelectronics and Materials, vol. 16, no. 1, pp. 135-144, 2023.

[45] M. Shkir, Z. R. Khan, A. Khan, K. V. Chandekar, M. A. Sayed, and S. AlFaify, "A Comprehensive Study on Structure, Opto-Nonlinear and Photoluminescence Properties of Co3O4 Nanostructured Thin Films: An Effect of Gd Doping Concentrations," Ceramics International, vol. 48, no. 10, pp. 14550-14559, 2022.

[46] O. A. Akintayo, G. M. Al-Senani, Y. A. Ajayeoba, S. D. Al-Qahtani, and S. A. Adewinbi, "Electrolytic Ion Diffusion Properties and Their Effects on Charge Storage Potentials of Pseudocapacitive Co3O4 Electrode Film," Ionics, vol. 31, no. 1, pp. 587-600, 2025.

[47] A. A. Khadayeir, E. S. Hassan, S. S. Chiad, N. F. Habubi, K. H. Abass, M. H. Rahid, Tahseen Hussain Mubarak, M. O. Dawood, and I. A. Al-Baidhany, "Structural and Optical Properties of Boron Doped Cadmium Oxide," Journal of Physics: Conference Series, vol. 1234, no. 1, 012014, 2019.

[48] M. Bouziani, A. Bouziani, A. Hsini, C. L. Bianchi, E. Falletta, A. Di Michele, et al., and R. Hausler, "Synergistic Photocatalytic Degradation of Methylene Blue and Ibuprofen Using Co3O4-Decorated Hexagonal Boron Nitride (hBN) Composites Under Sun-Like Irradiation," Chemosphere, vol. 371, 144061, 2025.

[49] P. Tukur, F. Tukur, S. Mantripragada, M. Saed, T. Nazifa, M. Liu, et al., and J. Wei, "Dynamic Active Site Reconstruction Dictates the Oxygen Evolution Reaction Performance of Cobalt-Based Electrocatalysts," Journal of Colloid and Interface Science, 139713, 2025.

[50] P. Goswami and G. Gupta, "Recent Progress of Flexible NO2 and NH3 Gas Sensors Based on Transition Metal Dichalcogenides for Room Temperature Sensing," Materials Today Chemistry, vol. 23, 100726, 2022.

[51] M. Gao, W. Zhang, J. Guo, and L. Liu, "Gas Sensor Based on Two-Dimensional GaSe for Sensitive NO2 Detection," Sensors and Actuators B: Chemical, vol. 444, 138447, 2025.

[52] S. Wei, Z. Li, K. Murugappan, Z. Li, F. Zhang, A. G. Saraswathyvilasam, et al., and L. Fu, "A Self-Powered Portable Nanowire Array Gas Sensor for Dynamic NO2 Monitoring at Room Temperature," Advanced Materials, vol. 35, no. 12, 2207199, 2023.

[53] H. AlQahtani, M. Alshammari, A. M. Kamal, and M. Grell, "Copper Phthalocyanine Chemiresistors as Industrial NO2 Alarms," Sensors, vol. 25, no. 9, p. 2955, 2025.

[54] F. S. Ahmed, N. Y. Ahmed, R. S. Ali, N. F. Habubi, K. H. Abass, and S. S. Chiad, "Effects of Substrate Type on Some Optical and Dispersion Properties of Sprayed CdO Thin Films," NeuroQuantology, vol. 18, no. 3, pp. 56-65, 2020.

[55] S. S. Chiad, K. H. Abass, Tahseen Hussain Mubarak, N. F. Habubi, M. K. Mohammed, and A. A. Khadayeir, "Fabrication and Study the Structure, Optical and Dispersion Parameters of PMMA with InCl3 Additive," Journal of Global Pharma Technology, vol. 11, no. 4, pp. 369-375, 2019.

[56] K. M. Girish, R. Lavanya, N. Sowmyshree, K. D. Jain, K. Gurushantha, and T. Ramakrishnappa, "Preparation and Electrochemical Properties of Co3O4 as Potential Electrode Materials for Supercapacitor and Battery Applications," Future Batteries, vol. 6, 100071, 2025.

[57] D. P. Shaik, M. S. Kumar, P. N. K. Reddy, and O. M. Hussain, "High Electrochemical Performance of Spinel Mn3O4 over Co3O4 Nanocrystals," Journal of Molecular Structure, vol. 1241, 130619, 2021.

[58] S. S. Nair, S. K. G, A. S. Pillai, and P. S. S, "Recent Advances in Co3O4 Based Nanocomposites for Supercapacitor Applications: A Comprehensive Review," Journal of Energy Storage, vol. 82, 110452, 2024.

[59] L. Zhang, Y. Liu, and X. Chen, "Room-Temperature Gas Sensors Based on Co3O4 Nanostructures: A Review of Recent Advances," Sensors and Actuators B: Chemical, vol. 398, 134726, 2024.

[60] M. A. K. Yousaf, M. Imran, and S. M. Abbas, "Tuning the Optical Bandgap of Co3O4 Thin Films via Transition Metal Doping for Optoelectronic Applications," Optical Materials, vol. 147, 114689, 2024.